Journal of Applied Polymer Science

Thermal, Mechanical, and Gas Barrier Properties of Ethylene-Vinyl Alcohol Copolymer-Based Nanocomposites for Food Packaging Films: Effects of Nanoclay Loading

Seong Woo Kim, Sang-Ho Cha
Department of Chemical Engineering, Kyonggi University, 94-6 Yiui-dong Yeongton-gu, Suwon, Gyeonggi-do 443-760, South Korea
Correspondence to: S. W. Kim (E - mail: wookim@kyonggi.ac.kr)

ABSTRACT: For the application of single-layer food packaging films with improved barrier properties, an attempt was made to prepare ethylene-vinyl alcohol (EVOH) copolymer-based nanocomposite films by incorporation of organically modified montmorillonite nanoclays via a two-step mixing process and solvent cast method. The highly intercalated tactoids coexisted with exfoliated clay nanosheets, and the extent of intercalation and exfoliation depended significantly on the level of clay loadings, which were confirmed from both XRD measurements and TEM observations. It was revealed that the inclusion of nanoclay up to an appropriate level of content resulted in a remarkable enhancement in the thermal, mechanical (tensile strength/modulus), optical, and barrier properties of the prepared EVOH/clay nanocomposite films. However, excess clay loadings gave rise to a reduction in the tensile properties (strength/modulus/elongation) and optical transparency due to the formation of clay tactoids with a larger domain size. With the addition of only 3 wt % clay, the oxygen and water vapor barrier performances of the nanocomposite films were substantially improved by 59 and 90%, respectively, compared to the performances of the neat EVOH film. In addition, the presence of clay nanosheets in the EVOH matrix was found to significantly suppress the moisture-derived deterioration in the oxygen barrier performance, implying the feasibility of applying the nanocomposite films to single-layer food packaging films. © 2013 Wiley Periodicals, Inc. J. Appl. Polym. Sci. **2014**, *131*, 40289.

KEYWORDS: EVOH/clay nanocomposites; barrier property; packaging film

Received 14 November 2013; accepted 10 December 2013
DOI: 10.1002/app.40289

INTRODUCTION

One of the most important properties of plastic packaging materials for food and medicine is an ability to protect the products against oxygen and moisture.[1] Nowadays, polyvinylidene chloride (PVDC) coated BOPP (biaxially oriented polypropylene) films with high gas barrier performance are widely used for food packaging because they serve as a good barrier against both oxygen and water vapor. Such high barrier performance can be originated from PVDC exhibiting very low oxygen and water vapor permeability values of around 0.064 cm^3 mm^{-1} m^{-2} day^{-1} atm^{-1} and 0.09 g mm^{-1} m^{-2} day^{-1}, respectively.[2] Recently, many research works have been conducted to develop chlorine free packaging films since chlorine causes environmental problems such as the generation of dioxins during incineration.[3] The cellulose nanofiber film prepared from natural plant cellulose as renewable biomaterial has recently drawn much attention due to its unique characteristics, especially excellent gas barrier performance. The research to overcome some problems involved in the process of converting native cellulose fibers into individual cellulose nanofibers, such as reduction of nanofiber length and low yields, has been performed for the application of flexible display panels as well as biodegradable packaging films with high gas barrier properties.[4,5] In addition, studies on the synthesis of chlorine free films using ethylene-vinyl alcohol copolymer (EVOH) show promising results in terms of gas barrier properties in dry conditions.[6,7] The commercially available EVOH grades contain 56–73 mol % vinyl alcohol. The excellent barrier properties of EVOH are attributed to the high cohesive energy density of the resin arising from the denser inter and intra molecular hydrogen bonding.[2] However, absorbed water reacts with the hydroxyl groups of the EVOH under humid atmospheres, resulting in deterioration in the gas barrier performance as well as the physical properties of the films, which is due to the plasticization of the EVOH copolymer chains.[8,9]

Therefore, hygroscopic EVOH film is usually sandwiched between high moisture barrier polyolefin layers via coextrusion

or lamination process to protect EVOH. However, these multiple-layer composite films have a number of limitations including high production cost, difficulties in recycling, and a lack of transparency. Currently, diverse techniques have been proposed to overcome these limitations. The development of recyclable monolayer blend films consisting of EVOH and polyolefin resins has been reported by several researchers.[10–12] In these blend films, the improvement in oxygen barrier property as well as moisture resistance property could be achieved through the formation of the elongated laminar structure of the dispersed EVOH phase within the polyolefin matrices due to the orientation effect during a single extrusion process. Another approach to protect the moisture-sensitive EVOH was also attempted in our previous study.[13] We have incorporated inorganic nanostructured silica particles with superior moisture barrier performance into the EVOH phase using sol-gel technology. However, despite its excellent barrier performance, such hybrid material-based monolayer films can be easily cracked due to the very high stiffness of silica; thus the application of these hybrids is limited to the thin coating layers on the BOPP or PET (poly ethylene terephthalate) substrate.

Meanwhile, organic–inorganic nanocomposite materials in which organically modified clay nanosheets are dispersed in a polymer matrix have attracted considerable attention. Such polymer nanocomposites exhibit greatly enhanced gas barrier, thermal, and mechanical properties with the incorporation of very low amounts of clay, compared to those of neat polymers or conventional composites with micrometer scales.[14–17] It has been commonly observed that improvements in the properties of nanocomposites are more prominent when highly intercalated or exfoliated nanoclay platelets are homogeneously dispersed in the polymer matrix.[18–21]

In this study, the incorporation of montmorillonite (MMT) nanoclay platelets into EVOH copolymer is attempted not only to increase the gas permeation resistance by increasing the tortuous path in the prepared nanocomposites, but also to minimize the deterioration of the barrier performance caused by moisture absorption. The EVOH/clay nanocomposite films are prepared via a two-step mixing operation followed by a solution casting process. We observe the clay dispersion state, including the intercalated and exfoliated structure of the prepared nanocomposite films using X-ray diffraction and transmission electron microscopy. The correlation between the extent of clay loading and the resulting properties of the nanocomposites such as thermal, mechanical, optical, and gas barrier properties is explored. In addition, the effect of nanoclay inclusion on the suppression of moisture-derived deterioration in the oxygen barrier performance is also investigated in terms of measurement of permeability as a function of time for the EVOH/clay films exposed to a humid atmosphere.

EXPERIMENTAL

Materials

Poly(ethylene-*co*-vinyl alcohol) with 32 mol % ethylene content supplied by Kuraray was used as a matrix. Clay used in this study was Na^+-MMT modified with methyl tallow bis-2-hydroxyethyl quaternary ammonium (C30B, Southern Clay Products), and *N*,*N*-dimetylyacetamide (DMAc) from Sigma–Aldrich was used as a solvent for dissolving EVOH resin without further purification.

Preparation of EVOH/Clay Nanocomposites and Films

EVOH resin with a powdery form was dissolved in a DMAc solvent at 60°C for 60 min to obtain 10 wt % solution A, and the C30B nanoclays were also dispersed in DMAc via sonication for 30 min (solution B). Solutions A and B were mixed, and then sonicated for 30 min followed by mixed vigorously for another 30 min using a homogenizer at a rotation speed of 2000 rpm to obtain an EVOH/clay nanocomposite solution with a homogeneous clay dispersion. The prepared nanocomposite solution was cast onto a glass substrate in rectangular scale with the dimensions of 10 × 10 cm^2. The solvent was, then, evaporated at 40°C in a drying oven for 48 h and the film was dried again at 80°C for another 48 h in a vacuum oven. The film thickness was measured by micrometer (ID-C112B, Mitutoyo, Japan). The thickness was determined by averaging the data measured on five different locations in the film. The average thickness of EVOH/clay cast film prepared in this study was measured to be around 40 μm. The prepared films were revealed to be homogeneous with respect to thickness, and the thickness variation with the level of clay loading could not be detected in the EVOH/clay nanocomposites. When preparing the nanocomposite film, the incorporated clay content varied at 1, 3, 5, and 7 wt %, accordingly, the name of the samples were designated as EVCL-1, EVCL-3, EVCL-5, and EVCL-7, respectively. All of the dried samples were kept in a dessicator to prevent the moisture influence prior to performing characterization.

Characterization

The gallery distance between the stacked nanoclay layers and degree of intercalation or exfoliation in the nanocomposites was quantitatively determined using an X-ray diffractometer (D8-Discover, Bruker) with Cu Kα radiation operated at 40 kV and 150 mA. Samples were scanned in the range of 1°–10° at a scanning rate of 1.0° min^{-1}. The prepared EVOH/clay nanocomposite was analyzed as a film, while the pristine clay was analyzed as a powder. The basal spacing of the clay was determined from the position of the d_{001} peak in the X-ray diffraction (XRD) pattern using Bragg's law.

The clay dispersion state including the intercalated and exfoliated nanostructure in the nanocomposites was qualitatively observed using a transmission electron microscope (TEM, JEM-2100F, JEOL, Japan) at an accelerating voltage of 200 kV. The specimens with a thickness of about 100 nm for TEM observation were prepared by ultramicrotoming of the cured epoxies containing nanocomposite film with a diamond knife.

Thermal characteristics such as melting point and crystallization temperature of the nanocomposites were examined using differential scanning calorimetry (DSC7020, Seico). The sample was initially heated from room temperature to 230°C at a heating rate of 30°C min^{-1} and the temperature was held at 230°C for 5 min to eliminate the previous thermal history. Subsequently, the sample was cooled down to room temperature at a cooling rate of 10°C min^{-1} to obtain cooling thermograms exhibiting crystallization temperature, and second heated to 230°C at a

rate of 10°C min^{-1} to obtain heating thermograms. Thermal stability was investigated by thermogravimetric analysis (TGA) using an Exstar 6000-TG/DTA6100 instrument (Seiko, Japan). The sample was heated from room temperature to 800°C at a heating rate of 10°C min^{-1}. The optical transparency of the EVOH/clay film was measured using a visible spectrophotometer (Optizen 1412V, Mecasys, Korea) in the visible-light wavelength range of 400–800 nm. Tensile properties of the nanocomposite films were measured according to ASTM D638 by using an universal testing machine (QM100S, Qmesys) at a cross-head speed of 20 mm min^{-1}. The average value was determined from data obtained by testing ten samples with dimensions of 10 mm (width) × 100 mm (length).

The oxygen transmission rate (OTR) of the EVOH/clay film was measured according to ASTM D 3985 using an OX-TRAN 2/10 (MOCON). Two types of dried and moisture absorbed samples were used in the OTR measurement. The samples with different amounts of absorbed water were prepared by storing them in a container maintaining 100% relative humidity for different periods. The water vapor transmission rate was also measured with a Permatran-W 3/33 (MOCON), of which the test method is based on ASTM F1249.

RESULTS AND DISCUSSION

Dispersion of Clay in Nanocomposites

Achieving a high degree of intercalation and/or delamination of organoclay in the polymer matrix has been considered to be prerequisite for the preparation of high performance polymer nanocomposites.[15] In this study, therefore, the polymer solution-based two-step mixing process was employed to impart a high level of energy or shear stress onto the agglomerated nanoclay particles, and consequently to induce intercalated and exfoliated nanoclay platelets with a homogeneous dispersion within the EVOH matrix. Figure 1 shows the XRD patterns in the 2θ region of 1°–10° for the samples of pristine powdery clay C30B and corresponding EVOH/clay nanocomposite films with various clay loadings. The diffraction peak of the pristine C30B was found at $2\theta = 4.8°$, which corresponds to an interlayer basal (d_{001}) spacing of 1.84 nm. In the case of nanocomposite samples with clay loadings of 1, 3, and 5 wt %, however, this characteristic peak of C30B disappeared, and flat diffraction patterns without peak were observed; this indicates that the agglomerated clay particles were effectively expanded and exfoliated into individual nanosheets, ultimately leading to homogeneous clay dispersion in the matrix. In addition, such a flat diffraction pattern may originate from a layer disorder resulting from a collapse of the original silicate structure upon imposed shear stress, and extremely low clay loadings.[22] On the basis of only XRD patterns, therefore, it is very difficult to precisely elucidate the clay dispersion state including the intercalated or exfoliated structure of the nanocomposite exhibiting flat diffraction pattern. In such a case, TEM observation is generally required along with XRD analysis to determine the exact nanostructured morphology of the nanocomposite. On the other hand, in the case where a nanocomposite contains a larger amount of clay (7 wt %), a single weak peak was observed at $2\theta = 4.5°$, which is lower than that corresponding to the characteristic peak of C30B, indicating the formation of intercalated clay tactoids with a slightly increased interlayer distance of 1.96 nm, along with exfoliated silicate layers. It was demonstrated from these XRD results that the clay dispersion nanostructure of the nanocomposite can be significantly influenced by the level of clay loadings, i.e., lower level of clay loading tends to yield a higher extent of intercalation or exfoliation structure with a homogeneous clay dispersion, which may be due to more effective energy or stress transfer onto agglomerated clay particles.

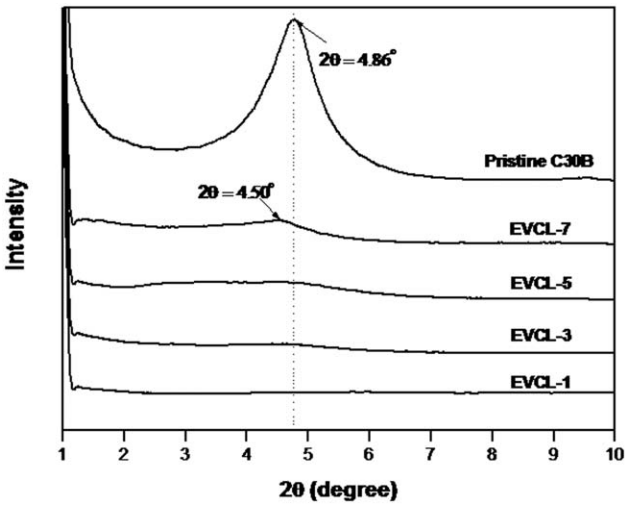

Figure 1. XRD patterns of pristine C30B and EVOH/clay nanocomposites with different clay loadings.

As mentioned earlier, a morphological observation by TEM was also performed to support the XRD results. Figure 2 shows the TEM images of the ultramicrotomed cross-sections of the nanocomposites with various clay loadings. The dark lines represent clay nanosheets of 1 nm thickness. As shown in the micrographs, the intercalated silicate tactoids with increased intergallery distance ranging from 2.2 to 3.7 nm and some exfoliated layers were observed to coexist in all of the nanocomposites samples regardless of clay loadings. Especially, when the clays were incorporated at a low content of 3 wt %, the fully exfoliated clay nanosheets were randomly dispersed in the matrix, and some intercalated tactoids consisting of only a few layers could also be detected. However, in the nanocomposite samples with an excess clay loading of 7 wt %, a high degree of intercalated tactoids, in which a larger number of silicate layers were stacked, were randomly distributed in the entire matrix, along with a low number of delaminated nanosheets. As confirmed in this TEM observation, a high degree of intercalation and exfoliation structure with a homogeneous clay dispersion in the EVOH/clay nanocomposites could be successfully achieved via the polymer solution-based two-step mixing process employed in this study. In addition, the strong hydrogen bonding, which is formed between the hydroxyl groups in the segments consisting of vinyl alcohol units in the EVOH copolymer and on the surface of C30B organoclay, seemed to accelerate the molecular diffusion of the EVOH into intergallery spaces between the clay platelets, ultimately resulting in a high degree of intercalation structure.

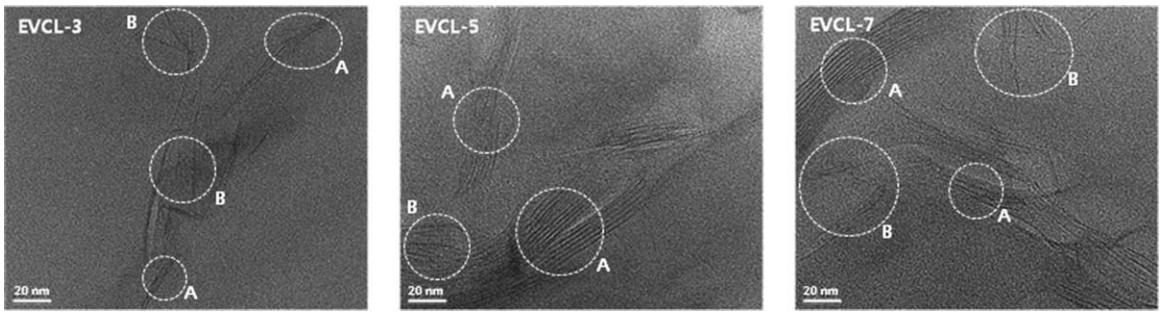

Figure 2. TEM images of EVOH/clay nanocomposites with different clay loadings. Character A designates the intercalated tactoids with a few layers and B exfoliated clay nanosheets.

Thermal Properties

The physical and mechanical properties of semicrystalline polymers are generally dependent on crystallization-derived molecular morphology.[23] In particular, the gas barrier performance determined by the rate of gas transport through the polymer is significantly influenced by both the degree of crystallinity and the crystalline structure developed in the semicrystalline polymer via the crystallization process. Accordingly, the crystallization behavior of the EVOH copolymer incorporated with nanoclay particles was examined in this study. Figure 3 shows the DSC cooling thermograms of neat EVOH and four EVOH/clay nanocomposites with various clay contents. Neat EVOH showed an exothermic peak at ca. 147°C, which corresponds to the crystallization temperature (T_c). In the case of EVOH/clay nanocomposites, the crystallization temperature was observed to increase with increasing clay content in the range of 1–7 wt %. The T_c of EVOH resin in the nanocomposite was increased by ca. 11°C by the incorporation of clay at 7 wt %, compared to that of neat EVOH. In this nanocomposite, the added nanoclay particles appeared to act as effective nucleating seeds, and thus increased the crystallization temperature of EVOH by promoting the overall crystallization rate, which is determined from the nucleation and crystal growth of the EVOH. The crystallization promoting effect caused by an incorporation of inorganic nano-sized particles has also been reported for the nanocomposites based on various crystalline polymers such as poly(lactic-acid), polypropylene, and polyamide.[24–27]

Inorganic micro- or nano-sized particles possessing superior heat resistant properties have been frequently used to enhance the thermal stability of organic polymers.[28,29] In this study, the effect of the incorporation of nanoclay particles on the thermal stability of EVOH-based nanocomposites was investigated in terms of TGA. Figure 4 shows the thermograms obtained from TGA for the neat EVOH and corresponding nanocomposites with different clay loadings. In the initial period of heating, the added organoclay gave rise to a higher rate of weight loss as shown in the inset of the figure, which seemed to deteriorate the thermal stability of the nanocomposite compared to neat EVOH. This result can be ascribed to the decomposition of low molecular weight organic modifiers (methyl tallow bis-2-hydroxyethyl quaternary ammonium) adsorbed on the clay surface. For the nanocomposites containing nanoclays treated with organic modifiers, the initial degradation temperatures have been usually observed to be reduced with increase of added nanoclay content because of decomposition phenomena of organic modifiers at initial low temperature range.[21,28] As the true thermal stability parameters, therefore, the degradation temperatures at 50% weight loss (T_{50}) were obtained from the

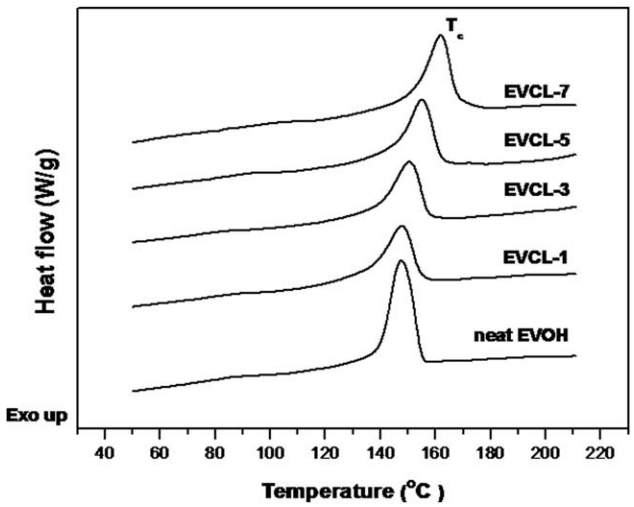

Figure 3. DSC cooling thermograms of neat EVOH and EVOH/clay nanocomposites with different clay loadings.

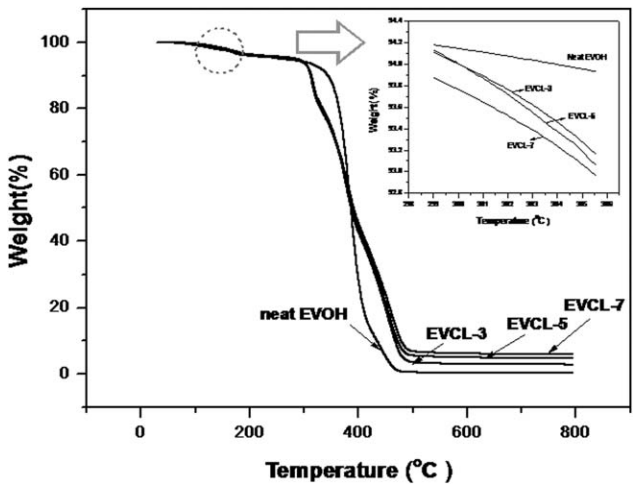

Figure 4. TGA thermograms of neat EVOH and EVOH/clay nanocomposites with different clay loadings.

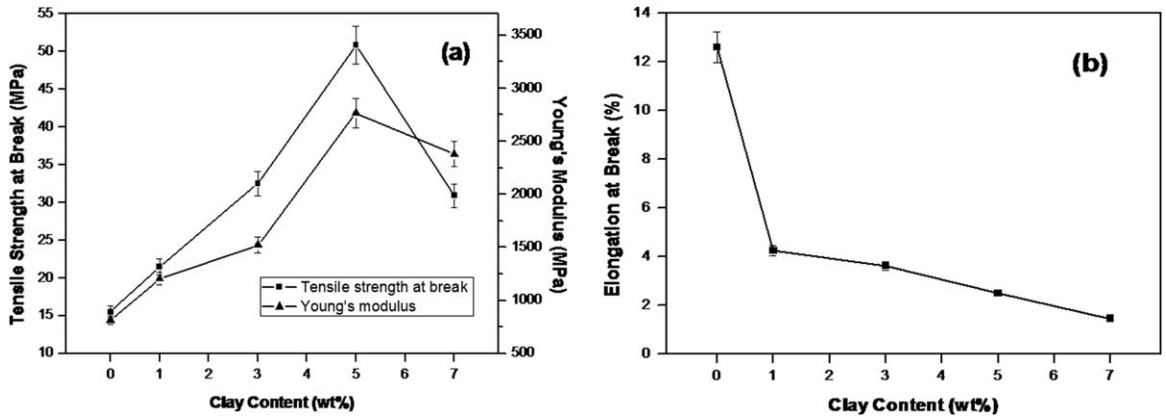

Figure 5. Tensile properties of EVOH/clay nanocomposite films as a function of clay content: (a) tensile strength at break and Young's modulus, (b) elongation at break.

thermograms in the higher temperature region after elimination of surfactants, which were determined as 386, 387, 389, and 392°C for the neat EVOH, EVCL3, EVCL5, and EVCL7, respectively. T_{50} increased by the addition of clay, and exhibited maximum rise for the nanocomposites with 7 wt % clay loading. This improvement in the thermal stability was due to the suppression of both heat transfer and oxygen permeation, which was caused by dispersion of clay nanosheets.[3]

Mechanical Properties

The tensile deformation test for the prepared nanocomposite casting films was performed to examine the mechanical reinforcing effect by the incorporation of clay in EVOH resin. Figure 5 shows the tensile properties of nanocomposite films as a function of clay content. The tensile strength at break and Young's modulus were remarkably improved with increasing clay content up to 5 wt %, and both exhibited a similar trend. However, when clays were added at 7 wt %, reductions in both tensile strength and modulus were observed. This deterioration in the mechanical property of the nanocomposite containing an excess amount of clay could be attributed to poor clay dispersion, which resulted from the occurrence of a larger number of stacked tactoids with greater domain size, as observed in the TEM image of Figure 5(c). On the other hand, elongation at break of the nanocomposite film decreased with an increasing of clay content in the entire range of 1–7 wt %; particularly, the reduction was most noticeable in the nanocomposite film with 1 wt % clay loading. Among the material properties, the stiffness is completely contrary to ductility. In tensile mechanical property, high modulus means the high degree of stiffness, and high elongation corresponds to high degree of ductility. An attempt to increase the modulus of the material will result in reduction in the elongation. Therefore, both tensile properties of modulus and elongation for the materials are not able to be improved simultaneously by only one technical method. It has been observed that the inclusion of inorganic clay possessing very high stiffness as well as high aspect ratio into polymer matrix improved the strength and modulus, but resulted in a reduction in the tensile elongation responsible for the flexibility of the nanocomposite film.[17,21]

In general, the flexible polymeric film is used for packaging film, because it usually undergoes various types of deformation including bending and wrapping during usage. Accordingly, we observed crack formation on the surface of the prepared nanocomposite films after bending test with 50 cycles. As a result, it could be confirmed that no crack occurred in the nanocomposite film. This implies that even the polymer nanocomposite film with only a few percent elongation has a capability enough to prevent crack formation by overcoming the stresses generated during bending or wrapping. Whereas, the polymer films coated with dense structure of SiO_x or SiO_2/polymer hybrids, have been reported to have a significant micro-crack problems.[13] For the application of practical packaging film, therefore, further study to impart an appropriate level of ductility to the stiff nanoclay-based nanocomposite film would be necessary. Blending with the ductile polymer resins such as polyurethane elastomer or low density polyethylene (LDPE) can be an alternative method to prepare the nanocomposite film with an appropriate level of flexibility. It should be noted that rigid crystalline films with low level of flexibility, such as biaxially oriented polypropylene (BOPP), poly(ethylene terephthalate), nylon, poly(lactic acid) films, are also used for the preparation of multi-layered packaging films.

Optical Transparency

Among the requirements for the application of food packaging film, high optical transparency is of great importance because it allows the condition of the food stored inside film, such as freshness or spoilage, to be clearly identified. In this study, the influence of clay addition on the optical transparencies of the nanocomposite films was investigated to present the feasibility of virtual application as a food packaging film. Figure 6 shows the relative light transmittance with respect to visible light in the wavelength range of 650–850 nm for the neat EVOH and nanocomposite films with various clay loadings. The light transmittance taken at specified wavelength above 600 nm has generally been presented as a representative value of it. To obtain clear graphical result, therefore, the light transmittance was measured in narrower range of 650–850 nm. Light transmittance increased with increasing clay content up to 5 wt %. Nanocomposite film with 5 wt % clay loading was highly transparent, transmitting around 92% of incident visible light in the investigated wavelength range, showing better transparency than neat EVOH film. This result suggests that the addition of

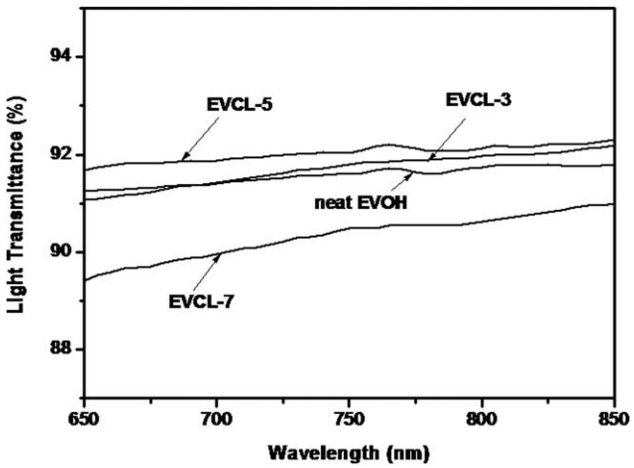

Figure 6. Light transmittance of neat EVOH and EVOH/clay nanocomposite films with different clay loadings.

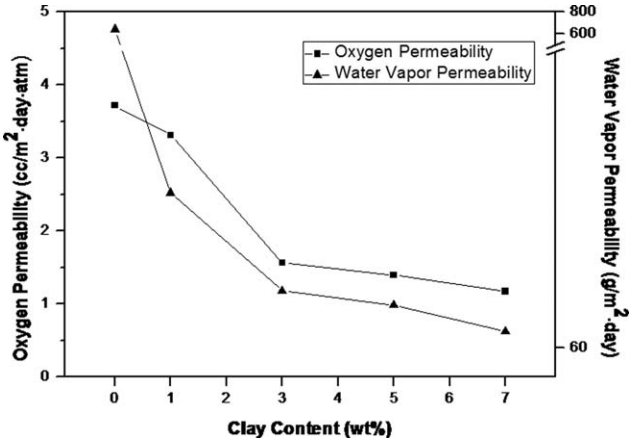

Figure 7. Oxygen and water vapor permeabilities of the EVOH/clay nanocomposite films as a function of clay content.

inorganic clays up to an appropriate content can yield highly transparent nanocomposite films to be utilized as food packaging films. Such an improvement in the optical transparency was believed to originate from the reduction in the degree of light scattering resulting from the decreased crystal size of the EVOH phase by the addition of clay particles. As observed in the above crystallization behavior, the size of EVOH spherulite that was formed via the crystallization process accompanied with solvent evaporation appeared to be reduced due to the presence of clay particles acting as a nucleating agent.[24,30] However, an excess amount of clay loading at 7 wt % resulted in a decrease in the light transmittance of the nanocomposite film, leading to poor transparency. This deterioration in transparency could be attributed to clay tactoids with a large domain size that were responsible for the high degree of light scattering, as confirmed in the TEM images.

Barrier Properties

The planar-structured nanoclay with high aspect ratio has been considered as an efficient barrier to the permeation of gas molecules such as oxygen, carbon dioxide, and water vapor. Accordingly, the incorporation of such inorganic clay nanoplatelets into a polymer matrix has been attempted to improve gas barrier performances of the produced nanocomposites by increasing the tortuous path for penetrating gases.[21,26,27] Figure 7 shows the oxygen and water vapor permeabilities of the EVOH/clay nanocomposite films plotted as a function of added clay content. The neat EVOH film had oxygen and water vapor permeabilities of 3.7 cm^3 m^{-2} day^{-1} atm^{-1} and 642.5 g m^{-2} day^{-1}, respectively. With an incorporation of 3 wt % clay, the oxygen and water vapor barrier properties of the nanocomposite films were dramatically improved by 59.4 and 90.1%, respectively, compared with neat EVOH film, exhibiting oxygen and water vapor permeabilities of 1.5 cm^3 m^{-2} day^{-1} atm^{-1} and 63.8 g m^{-2} day^{-1}, respectively. The improvement in the water vapor barrier property was shown to be more prominent compared to the oxygen barrier property. These considerable enhancements in both oxygen and water vapor barrier performances by the incorporation of only a small amount of clay (3 wt %) may be due to highly intercalated and delaminated clay nanoplatelets dispersed in the EVOH matrix. However, a further increase of clay content above 3 wt % was observed to have a minor effect on the improvement in both barrier properties, collectively showing the exponential decays in both permeabilities over the overall range of 1–7 wt % clay content.

Based on the identical film thickness of 40 μm, the EVOH/ clay (3 wt %) film prepared in this study exhibited much lower oxygen permeability (1.5 cm^3 m^{-2} day^{-1} atm^{-1}) as compared with biaxially oriented PP/EVOH blend film and PVDC/SiO_2 coated film with oxygen permeabilities of ~232.5 and ~63.0 cm^3 m^{-2} day^{-1} atm^{-1}, respectively, which had been reported in our previous work.[12,31] Such a considerable improvements in the barrier property of EVOH/clay nanocomposite over both blend and hybrid materials can be attributed to the homogeneous dispersion of delaminated planar-structured nanoplatelets with high aspect ratio, which is a significant factor in increasing the tortuous path for penetrating gas molecules within the polymer matrix. Owing to the spherical structure of incorporated silica particles, on the other hand, polymer/silica hybrid system has a limitation in the improvement of barrier property in spite of high loadings of them. Yeun et al.[3] have also reported that the oxygen permeabilities of poly(vinyl alcohol)-based hybrid films with 3 wt % nanoclay loading were shown to be ranging from 3.1 to 4.2 cm^3 m^{-2} day^{-1} atm^{-1}, depending on the nature of substrate used. These permeability values are somewhat higher than that of EVOH/clay (3 wt %) hybrid film prepared in this study. It can be believed that the discrepancy between these two oxygen permeabilities for different nanocomposite systems may be due to barrier characteristics of the polymer matrices (EVOH, PVA), clay dispersion structure, aspect ratio of used clay, and so on.

As mentioned earlier, EVOH has excellent oxygen and organic vapor barrier properties in dry conditions, but the barrier property deteriorates seriously in the presence of moisture because the absorbed water acts as a plasticizer, weakening the interchain forces in the polymer. In this study, therefore, we investigated the effect of clay incorporation on the variation in the oxygen barrier properties of the films which were exposed to humid atmosphere. Figure 8 shows the oxygen permeabilities of

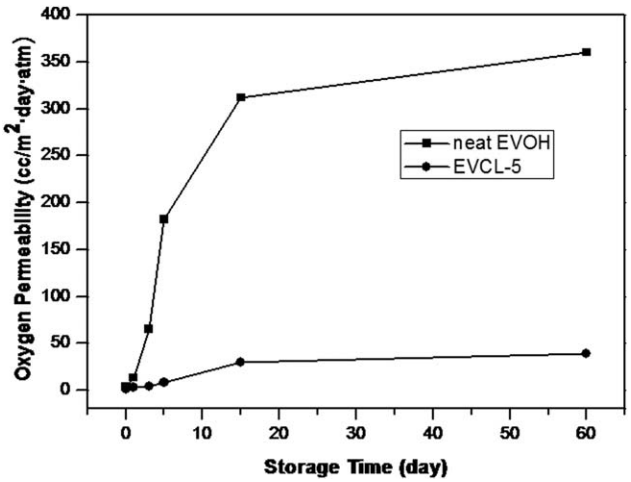

Figure 8. Oxygen permeabilities of neat EVOH and 5 wt % nanocomposite films as a function of storage time under humid atmosphere of 100% RH.

neat EVOH and 5 wt % nanocomposite films as a function of storage time under wet condition of 100% RH. The incorporation of 3 wt % clay resulted in the most prominent improvement in the barrier performance of the hybrid film. Considering the material cost, therefore, 3% nanocomposite film is advantage. However, we selected the 5% nanocomposite film to examine the humidity effect on the barrier property, because its oxygen permeability is lower than that of 3% nanoocmposite film, in spite of very small difference between them. Based on a comparison of oxygen permeability results for the neat EVOH and nanocompsite films, the presence of clay nanoplatelets in the EVOH matrix was found to significantly suppress the moisture-derived deterioration in the oxygen barrier performance, suggesting great potential for the application of moisture-sensitive EVOH film in the humid atmosphere. It can be believed that the highly intercalated and exfoliated clay nanosheets with high aspect ratios efficiently retarded the diffusion rate of water molecules within the EVOH matrix, ultimately minimizing the extent of reduction in the oxygen barrier properties of the films.

CONCLUSIONS

Organically modified montmorillonite nanoclays (C30B) were incorporated into EVOH resin to prepare nanocomposite films with improved physical and gas barrier performances. From XRD analysis and TEM observation, it was confirmed that a highly intercalated and exfoliated structure with a homogeneous clay dispersion in the EVOH matrix could be achieved, but the extent of intercalation and exfoliation was significantly influenced by the level of clay loadings. The thermal and mechanical properties (tensile strength/modulus), and optical transparencies of the nanocomposite films were revealed to be enhanced by an incorporation of nanoclays. However, tensile elongation properties were observed to be deteriorated due to stiffness of nanoclay itself, and excess clay loadings resulted in slight reduction in the tensile strength/modulus and light transmittance, which might be due to the formation of a larger number of intercalated clay tactoids with greater domain size. The prepared nanocomposite films showed substantially improved oxygen and water vapor barrier performances, compared with the neat EVOH film. The decreasing rate of permeation was observed to be more prominent in the low range of clay loadings. In addition, the presence of nanoclay platelets in the EVOH matrix significantly suppressed the moisture-induced deterioration in the oxygen barrier property by minimizing the moisture permeation rate, suggesting the feasibility of the application of moisture-sensitive EVOH resin for single-layer food packaging films.

ACKNOWLEDGMENTS

This research was supported by a grant from "Fusion Technology Development Program" of Korea Research Council Industrial Science and Technology.

REFERENCES

1. Iotti, M.; Fabbri, P; Messori, M. *Polym. Environ.* **2009**, *17*, 10.
2. Finch, C. A. Polyvinyl Alcohol; Wiley: New York, **1993**; Chapter *8*.
3. Yeun, J. H.; Bang, G. S.; Park, B. J.; Ham, S. K.; Chang, J. H. *J. Appl. Polym. Sci.* **2006**, *101*, 591.
4. Fukuzumi, H.; Saito, T.; Iwata, T.; Kumamoto, Y.; Isogai, A. *Biomacromolecules* **2009**, *10*, 162.
5. Aulin, C.; Gallstedt, M.; Lindstrom, T. *Cellulose* **2010**, *17*, 559.
6. Lopez-Carballo, G.; Cava, D.; Lagaron, J. M.; Catala, R.; Gavara, R. *J. Agric. Food Chem.* **2005**, *53*, 7212.
7. Lopez-Rubio, A.; Lagaron, J. M.; Hernandez-Munoz, P.; Almenar, E.; Catala, R.; Gavara, R.; Pascall, M. A. *Innovative Food Sci. Emerg. Technol.* **2005**, *6*, 51.
8. Muramatsu, M.; Okura, M.; Kuboyama, K.; Ougizawa, T.; Yamamoto, T.; Nishihara, Y.; Saito, Y.; Ito, K.; Kobayashi, Y. *Radiat. Phys. Chem.* **2003**, *68*, 561.
9. Zhang, Z.; Britt, I. J.; Tung, M. A. *J. Appl. Polym. Sci.* **2001**, *82*, 1866.
10. Lohfink, G. W.; Kamal, M. R. *Polym. Eng. Sci.* **1993**, *33*, 1404.
11. Faisant, J. B.; Kadi, A. A.; Bousmina, M.; Deschenes, L. *Polymer* **1998**, *39*, 533.
12. Yeo, J. H.; Lee, C. H.; Park, C. S.; Lee, K. J.; Nam, J. D.; Kim, S. W. *Adv. Polym. Tech.* **2001**, *20*, 191.
13. Nam, J. D.; Kim, S. W. *J. Appl. Polym. Sci.* **2010**, *115*, 1663.
14. Dan, C. H.; Lee, M. H.; Kim, Y. D.; Min, B. H.; Kim, J. H. *Polymer* **2006**, *47*, 6718.
15. Chavarria, F.; Paul, D. R. *Polymer* **2006**, *47*, 7760.
16. Ma, X.; Lu, H.; Liang, G.; Yan, H. *J. Appl. Polym. Sci.* **2004**, *93*, 608.
17. Jeong, H. M.; Kim, B. C.; Kim, E. H. *J. Mater. Sci.* **2005**, *40*, 3783.
18. Lee, S. K.; Seong, D. G.; Youn, J. R. *Fibers Polym.* **2005**, *6*, 289.

19. Chen, G.; Yoon, J. *Polym. Degrad. Stab.* **2005**, *88*, 206.
20. Krikorian, V.; Pochan, D. *J. Chem. Mater.* **2003**, *15*, 4317.
21. Cho, T. W.; Kim, S. W. *J. Appl. Polym. Sci.* **2011**, *121*, 1622.
22. Ray, S. S.; Yamada, K.; Okamoto, M.; Fujimoto, Y.; Ogami, A.; Ueda, K. *Polymer* **2003**, *44*, 6633.
23. Wu, D.; Wu, L.; Xu, B.; Zhang, Y.; Zhang, M. *J. Polym. Sci. B Polym. Phys.* **2007**, *45*, 1100.
24. Chow, W. S.; Lok, S. K. *J. Therm. Anal. Cal.* **2009**, *95*, 627.
25. Lee, J. H.; Park, T. G.; Park, S. H.; Lee, D. S.; Lee, Y. K.; Yoon, S. C.; Nam, J. D. *Biomaterials* **2003**, *24*, 2773.
26. Mirzadeh, A.; Kokabi, M. *Eur. Polym. J.* **2007**, *43*, 3757.
27. Jiang, T.; Wang, Y.; Yeh, J.; Fan, Z. *Eur. Polym. J.* **2005**, *41*, 459.
28. Chang, J. H.; An, Y. U. *J. Polym. Sci. B Polym. Phys.* **2002**, *40*, 670.
29. Chen, T. K.; Tien, Y. I.; Wei, K. H. *Polymer* **2000**, *41*, 1345.
30. Rosen, S. L. Fundamental Principles of Polymeric Materials, 2nd ed.; Wiley: New York, **1993**; p 50.
31. Hwang, T.; Pu, L.; Kim, S. W.; Oh, Y. S.; Nam, J. D. *J. Membr. Sci.* **2009**, *345*, 90.